Measurement of homonuclear three-bond $J(H^NH^\alpha)$ coupling constants in unlabeled peptides complexed with labeled proteins: Application to a decapeptide inhibitor bound to the proteinase domain of the NS3 protein of hepatitis C virus (HCV)

Daniel O. Cicero, Gaetano Barbato, Uwe Koch, Paolo Ingallinella, Elisabetta Bianchi, Sonia Sambucini, Petra Neddermann, Raffaele De Francesco, Antonello Pessi & Renzo Bazzo* *IRBM P. Angeletti, via Pontina km 30.600, I-00040 Pomezia (Rome), Italy*

Received 30 October 2000; Accepted 12 February 2001

Key words: coupling constants, HCV, HNHA, isotope filtering, NS3

Abstract

A new isotope-filtered experiment has been designed to measure homonuclear three-bond $J(H^NH^\alpha)$ coupling constants of unlabeled peptides complexed with labeled proteins. The new experiment is based on the 3D HNHA pulse scheme, and belongs to the 'quantitative J-correlation' type. It has been applied to a decapeptide inhibitor bound to the proteinase domain of the NS3 protein of human hepatitis C virus (HCV).

Introduction

In our program of structure determination of complexes between the proteinase domain of the NS3 protein of human hepatitis C virus (HCV) and inhibitors (Cicero et al., 1999; Barbato et al., 2000), we have recently focused our attention on P775 (Ac-AspGluLeuIleChaCysProChaAspLeu-NH₂, where Glu is the D-amino acid and Cha stands for cyclohexylalanine), a decapeptide inhibitor which was obtained from natural substrates by introducing a proline residue in position P1' to make it non-cleavable¹ (Ingallinella et al., 2000). The amino acid sequence of P775 has been optimized for binding by screening peptide libraries, leading to an inhibitor with an IC₅₀<200 pM (Ingallinella et al., 2000). The structure of the complex between the proteinase domain of NS3 and P775 (P775/NS3-protease, MW 22.0 kDa)

One important step for the structure determination of the complex is the measurement of the vicinal proton-proton couplings between amide and alpha protons. Qualitatively, they give information on the secondary structure and if accurate values are available, they can be translated, via the Karplus equation (Karplus, 1959; Bystrov, 1976; Vuister and Bax, 1993), into structural constraints for Φ-dihedral angles. These parameters cannot be measured from 1D NMR spectra, due to the linewidth and the overlap of protein resonances. Therefore several methods have been developed for the measurement of NH-Hα coupling constants in labeled proteins. Different approaches, like the HMQC-J experiment (Forman-Kay et al., 1990; Kay et al., 1990; Heikkinen et al., 1999), methods based on multiple-quantum coherences (Rexroth et al., 1995) and the HNCA-J experiment (Madsen et al., 1993; Weisemann et al., 1994; Löhr and Rüterjans, 1995), extract the coupling constant values from a frequency difference between two signals modulated by $J(H^NH^{\alpha})$. On the other hand, the so-called 'quantitative J-correlation experiments' measure the coupling constant of interest from peak

can give insights that may be relevant for the drug discovery process.

^{*}To whom correspondence should be addressed. E-mail: renzo_bazzo@merck.com

¹We follow the nomenclature proposed by Schechter and Berger (1967) whereby the cleavage site is designated as P6-P5-P4-P3-P2-P1... P1'-P2'-P3'-P4' etc., with the scissile bond located between P1 and P1' and the C-terminus of the substrate on the prime side.

intensities. They include the HNHA (Kuboniwa et al., 1992; Vuister and Bax, 1993), the J-modulated HSQC (Billeter et al., 1992) and the intensity-modulated HSQC and HMQC experiments (Permi et al., 2000). Due to their relative simplicity and accuracy, these methods, based on peak intensities, are the most frequently used for measuring $J(H^NH^\alpha)$. A common condition for the application of all these methods is the availability of a labeled (^{15}N or ^{15}N , ^{13}C) polypeptide chain.

In view of the significant impact that constraints derived from $J(H^NH^\alpha)$ can have on the structure refinement process, we have implemented a 2D isotope-filtered version of the HNHA experiment (Vuister and Bax, 1993) to measure $J(H^NH^\alpha)$ couplings for the unlabeled peptide. Since the signals of the labeled protein are completely removed from the spectrum by an extensive isotope-filtering procedure, one can easily determine the $J(H^NH^\alpha)$ coupling constants of the bound peptide. The pulse sequence is similar to the one proposed for measuring H^α - H^β J coupling constants of specific residues in proteins, using the so-called 'reverse isotopic labeling' method (Vuister et al., 1994). Our pulse sequence applies generally to all bound unlabeled ligands.

Materials and methods

The 15 N, 13 C-labeled protease domain of the HCV BK strain NS3 protein (amino acids $1027{-}1206$, followed by AlaSerLysLysLysLys) was expressed in *E. coli* and purified as previously described (Barbato et al., 1999). P775 was prepared by solid phase synthesis using Fmoc-t-Bu chemistry (Ingallinella et al., 2000). The concentration of the complex was around 800 μ M. The final buffer contained 20 mM sodium phosphate, 3 mM dithiothreitol, 0.1% of Triton, 5 mM NaN₃, pH 6.6.

All NMR experiments were acquired at 300 K on a Bruker Avance 600 MHz spectrometer equipped with a z-shielded gradient triple resonance probe. Spectral assignments of P775 bound to NS3 protease domain were obtained using the 2D isotope-filtered versions of TOCSY and NOESY experiments (Ikura and Bax, 1992; Dalvit et al., 1999) and the N,C-filtered HNHA experiments described here. ¹⁵N T₁ and T₂ relaxation measurements were performed by the sequences described by Farrow et al. (1994). ¹⁵N T_{1zz} relaxation measurements were done using the experiment de-

scribed by Kay et al. (1992), introducing flip-back and field gradient pulses to minimize solvent saturation.

The calculations and numerical integrations were performed using the D02BBF NAG FORTRAN Library Routine (Nag Ltd, Oxford, UK).

Peak intensity measurement and $J(H^NH^\alpha)$ calculation If the amide spin is described by an operator I^N and the H^α spin by I^α , the application of pulse sequences based on the HNHA experiment (Vuister and Bax, 1993) produces both a diagonal peak, originating from the in-phase component I_y^N , and a cross peak, arising from the antiphase magnetization $2I_x^NI_z^\alpha$. In a first approximation, the intensity ratio between the cross peak (S_{cross}) and the diagonal peak (S_{diag}) provides a direct measure for the magnitude of J_{HH} (Vuister and Bax, 1993):

$$S_{cross} / S_{diag} = -\tan^2 (2\pi J_{HH} \zeta)$$
 (1)

In deriving Equation 1, we have assumed that the magnetization components that give rise to diagonal and cross peaks relax at identical rates during the dephasing and refocussing delays. However, since the antiphase magnetization relaxes somewhat faster than the in-phase component (Lynden-Bell, 1967; Harbison, 1993), the application of Equation 1 leads to an underestimation of the coupling constants. More accurate results can be obtained by solving the corresponding differential equation system (Vuister and Bax, 1993), by an appropriate numerical routine:

$$d\left\langle I_{y}^{N}\right\rangle /dt = \pi J_{HH} \left\langle 2I_{x}^{N}I_{z}^{\alpha}\right\rangle - \left\langle I_{y}^{N}\right\rangle /T_{2HN} \qquad (2a)$$

$$\begin{array}{c} d\left\langle 2I_{x}^{N}I_{z}^{\alpha}\right\rangle /dt\!=\!-\pi J_{HH}\left\langle I_{y}^{N}\right\rangle \!-\!\left\langle 2I_{x}^{N}I_{z}^{\alpha}\right\rangle /T_{2HN} \\ -\left\langle 2I_{x}^{N}I_{z}^{\alpha}\right\rangle /T_{1sel} \end{array} \tag{2b}$$

where $J_{HH}=J(H^NH^\alpha),~T_{2HN}$ is the transverse relaxation time of the in-phase H^N magnetization and T_{1sel} describes the apparent selective T_1 of the H^α spin, or spin flip relaxation time. By numerical integration between t=0 and $t=2\zeta$ one can calculate the $\langle 2I_x^NI_z^\alpha\rangle/\left\langle I_y^N\right\rangle$ ratio. On the other hand, the experimental value of S_{cross}/S_{diag} at time $t=2\zeta$ corresponds to $\{\langle 2I_x^NI_z^\alpha\rangle/\left\langle I_y^N\right\rangle\}^2$. The $\langle 2I_x^NI_z^\alpha\rangle/\left\langle I_y^N\right\rangle$ ratio does not depend on the exact value of T_{2HN} and therefore T_{1sel} remains the only relaxation time parameter one has to include explicitly to integrate the equation system. Usually a single value of T_{1sel} can be assumed for all peaks, to a very good approximation (Vuister and Bax, 1993). To avoid the need of a separate evaluation of

 T_{1sel} one can perform the experiment for two values of the total time $t=2\zeta$. The 'best' values of T_{1sel} and J_{HH} are then computed as those values that maximize the agreement or 'matching' (Cicero et al., 1995) between calculated (by Equation 2) and experimental values of peak intensities.

The resulting value for T_{1sel} can then be compared with estimations derived from relaxation measurements. In fact, if we assume that the spin flip rate is almost linearly proportional to the isotropic rotational correlation time τ_c of the protein (Vuister and Bax, 1993; Kuboniwa et al., 1994; Ponstingl and Otting, 1998), a correction coefficient can be calculated once τ_c is known (Permi et al., 2000). Taking as a reference the value of T_{1sel} used for staphylococcal nuclease (SNase, MW 17.5 kDa, $\tau_c = 9$ ns) (Kay et al., 1992), which was 100 ms, one can derive the following empirical relationship:

$$1/T_{1sel} \approx 1.11 \cdot 10^9 \text{ s}^{-2} \tau_c$$
 (3)

On the other hand, it is possible to estimate T_{1sel} from separate experiments which measure the decay of I_zS_z and S_z terms (Vuister and Bax, 1993). A direct measurement is feasible only if a $^{13}C^{\alpha}$ selectively labeled protein is available. If this is not the case, one can calculate T_{1sel} for amide protons and consider those as an estimate of the value expected for the H^{α} spin flip relaxation time.

Since all these approaches have an associated uncertainty, we have adopted all three, and compared the results.

Results and discussion

Pulse sequence description

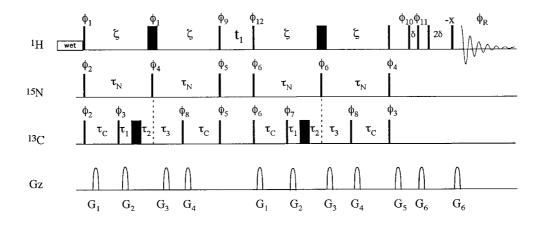
Two versions of the N,C-filtered HNHA experiment are presented in Figure 1. These experiments are based on the 3D HNHA experiment (Vuister and Bax, 1993), which relies on the quantitative estimation of the diagonal peak to cross peak intensity ratio in a H^N - H^α homonuclear J correlation experiment. Experiments in Figure 1 differ from the original sequence in that the long period used to transfer magnetization from the H^N to the H^α nucleus (10.6 ms in experiment 1a, 21.2 ms in experiment 1b) is employed to eliminate signals arising from ^{15}N - or ^{13}C -bound protons, instead of monitoring the frequency of the attached ^{15}N spin. In this way, only signals originating from the unlabeled peptide will survive the extensive filtering

procedure, yielding a 2D spectrum of the unlabeled peptide that can be used for the J calculation. The isotope filtering is achieved by a combination of purge filters (Kogler et al., 1983; Ikura and Bax, 1992) and pulse field gradients (Keeler et al., 1994; Dalvit et al., 1999). In this scheme, the purging is obtained by conversion of proton heteronuclear antiphase magnetizations of the protein into heteronuclear multiplequantum (MQ) coherences. Such components get completely dephased by gradients and consequently become not observable. Taking advantage of the long delay used for H^N - H^α coupling evolution, the isotopic filters can be applied several times (4 times for ¹⁵Nfiltering and 6 times for ¹³C-filtering in sequence 1a, 8 times for ¹⁵N-filtering and 12 times for ¹³C-filtering in sequence 1b). Such extensive filtering guarantees an excellent suppression of signals of protons attached to ¹⁵N or ¹³C spins. The carbon carrier was positioned in the aromatic region, and the delay τ_C was chosen to match the ¹J_{HC} usually found in aromatic side chains (~ 160 Hz), whose signals could overlap with the amide proton signals of the peptide (6 to 12 ppm).

Application of the N,C-filtered HNHA experiment to the P775/NS3-protease complex

Both experiments 1a ($2\zeta = 10.6$ ms) and 1b ($2\zeta =$ 21.2 ms) were applied to a sample of the complex formed by unlabeled P775 and ¹⁵N, ¹³C-labeled NS3protease. As an example of the results obtained, Figure 2 shows a section of the 2D spectrum of P775/NS3-protease using sequence 1b. Eight out of the nine HN-Ha cross peaks expected for P775 are observed. Only the P1 H^N - H^{α} correlation is missing, due to very unfavorable relaxation. The suppression of the labeled protein resonances is virtually complete, since no residual signal splitted in both dimensions by the heteronuclear couplings is visible in the spectrum. Only two cross peaks not belonging to P775 are present, one from an impurity of the detergent (peak x), and the H^N - H^{α} cross peak of the very slow relaxing C-terminal residue (K186) of the residual unlabeled NS3 (peak xx). K186 is actually the last residue of the solubilizing tail (ASKKKK) and, due to its exceptional mobility (backbone ¹⁵N T₂ for K186 is about 10 times longer compared to the protein average), it exhibits a very long ¹H T₂ value. For this reason the residual unlabeled fraction of K186, in spite of its small amount (< 2%), shows up in the spectrum. However, this result underlies a potential source of inaccuracies since any unlabeled compound with very slow ¹H T₂ relaxation could give a residual signal,

a $(2\zeta=10.6 \text{ ms})$



b (2ζ=21.2 ms)

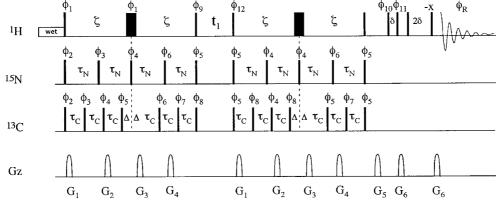


Figure 1. Pulse schemes of the N,C-filtered HNHA experiment with (a) 10.6 ms and (b) 21.2 ms of magnetization transfer delay between HN and Hα protons. Narrow and wide pulses correspond to 90° and 180° flip angles, respectively, and were applied along the x-axis unless indicated otherwise. Solvent suppression was achieved by a combination of a WET scheme (Smallcombe et al., 1995), and a spin-echo water suppression sequence (Sklenář and Bax, 1987). The following phase cycle was used for both experiments: $\phi_1 = x, -x; \phi_2 = 64x, 64(-x); \phi_3 = 128x, 128(-x); \phi_4 = 256x, 256(-x); \phi_5 = 16x, 16(-x); \phi_6 = 32x, 32(-x); \phi_7 = 64x, 64(-x); \phi_8 = 256x, 256(-x); \phi_9 = 8y, 8(-y); \phi_{10} = 2x, 2y, 2(-x), 2(-y); \phi_{11} = 2(-x), 2(-y), 2x, 2y; \phi_{12} = 16y, 16(-y); \phi_R = x, -x, -y, y, -x, x, y, -y. Quadrature detection in t₁ was obtained with the States-TPPI method incrementing phases <math>\phi_1$ and ϕ_9 . Delays are: $\tau_N = 5.3$ ms; $\tau_C = 3.2$ ms; $\tau_1 = 1.6$ ms; $\tau_2 = 0.5$ ms; $\tau_3 = 2.1$ ms; $\Delta = 1.0$ ms; $\delta = 117$ μs. Delay ζ is equal to τ_N (scheme (a)) or $2\tau_N$ (scheme (b)). All gradients have a duration of 800 μs, and are sine-bell shaped, with the following gradient strengths at their midpoint: $G_1 = 15$ G/cm; $G_2 = 25$ G/cm; $G_3 = 10$ G/cm; $G_{4,5} = 30$ G/cm; $G_6 = 40$ G/cm. For both experiments the carrier was positioned at the H₂O frequency during the WET scheme, shifted to 6.6 ppm before the first proton hard pulse, and returned to the H₂O frequency before the spin-echo jump-return pulses.

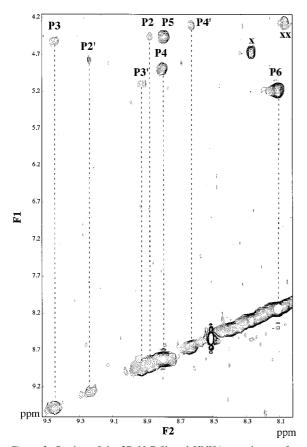


Figure 2. Section of the 2D N,C-filtered HNHA experiment of a complex between $^{15}\text{N/}^{13}\text{C}$ labeled NS3-protease and unlabeled decapeptide inhibitor P775, recorded with pulse scheme 1b at 300 K. The spectrum results from 1024 scans per complex t_1 increment. The acquired data matrix contains 48 complex data points in the t_1 dimension. The FID acquisition time was 350 ms and the total measuring time about 40 h. Field strength was 600 MHz. The spectrum was zero-filled to yield digital resolutions of 14.5 (F_1) and 2.4 (F_2) Hz, after apodization with Lorentzian-to-Gaussian (F_2) and shifted cosine-bell (F_1) window functions. Resonances in the F1 region between 5.5 and 4.2 ppm are H^N -H $^{\alpha}$ cross peaks with negative intensities and resonances downfield of F1 = 7.7 ppm are H^N diagonal peaks with positive intensities.

even if present as an impurity at a very low concentration, since the long delay used in the pulse sequence is bound to penalize the faster relaxing signals of the bound ligand. During such a delay, though, the signal intensities of fast diffusing small molecules can be reduced by the use of gradients. As a result, in our case residual spurious signals are only visible on the diagonal and they do not significantly affect the determination of the ligand peak intensities.

In Table 1 we report the measured values for S_{cross}/S_{diag} obtained on the P775/NS3-protease complex, using sequences 1a and 1b. The reported errors

Table 1. Cross peak to diagonal peak intensity ratio (S_{cross}/S_{diag}) measured for unlabeled P775 complexed with $^{15}N,^{13}C$ -labeled NS3-protease at two different dephasing periods 2 ς of the N,C-filtered HNHA experiment

Residue	Scross/Sdiag	
	$2\zeta = 10.6 \text{ ms}$	$2\zeta = 21.2 \text{ ms}$
P6	-0.078 ± 0.003	-0.323 ± 0.004
P5 ^a	-0.026 ± 0.004	-0.107 ± 0.011
P4 ^a	-0.029 ± 0.004	-0.115 ± 0.010
P3	-0.076 ± 0.017	-0.366 ± 0.064
P2	-0.037 ± 0.013	-0.152 ± 0.038
P2'	n.d.	-0.452 ± 0.110
P3'	-0.031 ± 0.012	-0.142 ± 0.034
P4'	-0.028 ± 0.010	-0.144 ± 0.031

^aWhen the diagonal peaks are overlapped, the value reported is the ratio between the cross peak and the sum of the two diagonal peaks.

Table 2. $J(H^NH^\alpha)$ coupling constants for P775 in the P775/NS3 complex, obtained from the N,C-filtered HNHA experiment

Residue	$J(H^NH^\alpha)\ (Hz)$
P6	8.7±0.4
P5	7.2 ± 0.3
P4	7.6 ± 0.3
P3	8.9 ± 0.3
P2	6.2 ± 0.3
P2'	9.9 ± 0.5
P3'	5.9 ± 0.2
P4'	5.8 ± 0.2

were calculated by estimating the average noise intensity in regions of the spectrum where no peaks were detected. The interference on diagonal peaks of residual spurious signals was also evaluated and included, although the corresponding error turned out to be comparatively small. Finally the standard error propagation theory has been applied to work out the estimated errors on the peak intensity ratios.

Equations 2a and b were then used to calculate the expected values for S_{cross}/S_{diag} at time $t=2\zeta$ for a given value of T_{1sel} . The use of peak intensities, rather than integrals, is justified by the apparent linewidth in F_1 being determined almost exclusively by the apodization function. On the other hand, different linewidths in F_2 do not need to be considered since their effect drops out in the ratios, except for

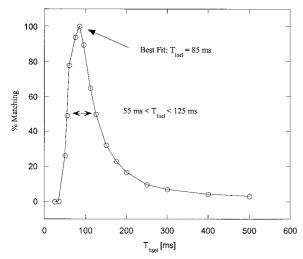


Figure 3. Matching curve for the estimation of T_{1sel} from the peak intensity ratios of Table 1. See text for definition of M. At a given value of T_{1sel} , the set of $J(H^NH^\alpha)$ for all the residues is calculated that maximizes the value of M (see Equation 4).

overlapping peaks. In fact, for residues P5 and P4, the H^N chemical shift is almost identical, therefore only the sum of the intensities of the two diagonal peaks can be measured. One can, however, use the individual cross peak intensities and the sum of the two diagonal peaks to calculate both coupling constants if one assumes the same linewidth in F_2 for these two residues. A simple inspection of the relative signal linewidths in F_2 (using of course a sufficient signal resolution in observation) would, however, be sufficient to evaluate a correction factor, if needed. For these residues the calculated parameters are $S_{cross(P4)}/(S_{diag(P4)}+S_{diag(P5)})$ and $S_{cross(P5)}/(S_{diag(P4)}+S_{diag(P5)})$. The corresponding values are listed in Table 1.

To obtain the values of T_{1sel} that best reproduce the peak intensity ratios observed, the matching curve for T_{1sel} was calculated (Cicero et al., 1995). The graphic in Figure 3 was generated by assuming a given value of T_{1sel} , and calculating the set of $J(H^NH^\alpha)$ values (one for each residue) that maximize the matching M with the experimental data. The matching M is defined as follows (Cicero et al., 1995):

$$M = \prod_{i} exp - \left\{ 1/2 \left[\left(A_{i}^{exp} - A_{i}^{calc} \right) / \Delta A_{i} \right]^{2} \right\}$$
 (4)

where A_i^{exp} and A_i^{calc} are the experimental and calculated parameters, respectively, and ΔA_i their corresponding errors. M is then reported as a function of T_{1sel} . Clearly, maximizing M is equivalent to minimizing the sum of the square differences between A_i^{exp}

and $A_{\rm i}^{\rm calc}$, weighted according to the estimated accuracy of each particular parameter. This analysis is of crucial importance when the errors associated with the measured variables are not homogeneous, as in the present case for peak intensities with variable signal to noise. We arbitrarily assigned 100% of matching to the solution that exhibits the highest value of M (the 'best fit' solution).

Inspection of the matching curve of Figure 3 shows that the 'best fit' solution occurs with $T_{1sel}=85~\text{ms},$ although values in the range 55 to 125 ms exhibit degrees of matching with experimental data higher than 50% . This interval (55 ms $\leq T_{1sel} \leq$ 125 ms) was then taken to define the region that contains with the highest probability the real value of T_{1sel} .

Independently, we have measured the $T_1,\,T_2$ and T_{1zz} relaxation times of ^{15}N of the amide groups of the labeled NS3 protein in the P775/NS3 complex. We considered only values of T_1/T_2 within one standard deviation from the average to estimate the correlation time τ_c of the molecule, as described earlier (Farrow et al., 1994). This approach provided a value for τ_c of 9.7 ns. By replacing this value of τ_c in Equation 3 one can estimate a value for T_{1sel} of \sim 93 ms, in good agreement with the 'best fit' solution of Figure 3.

On the other hand, an analysis of T_1 and T_{1zz} for the amide groups of NS3 in the complex provided average values of 800 ms and 70 ms, respectively (at 600 MHz). This would translate in a value for T_{1sel} of about 77 ms, again in very good agreement with the 'best fit' solution. However, it is important to emphasize that this T_{1sel} refers to the H^N spin, which can be slightly different from the T_{1sel} of the H^α proton that directly relates to the $J(H^NH^\alpha)$ measured in the HNHA experiment.

In view of these results, we have used a value of 85 ms for T_{1sel} to calculate the values of the $J(H^NH^\alpha)$ couplings for P775, which are listed in Table 2, and assumed an interval of confidence for each value corresponding to the region of good matching represented in Figure 3.

One does not need to emphasize the importance of these three-bond J couplings for determining the conformation of P775 bound to the NS3 protein. In general, our method allows a precise measurement of these parameters for unlabelled peptides bound to proteins of even substantial size and therefore represents the natural complement of the original experiment, designed to measure the same parameters for the labeled protein. In general, as is well known, the relative contribution of constraints like Φ -dihedral angles to

the definition of a 3D protein structure with respect, typically, to NOE data varies for different regions. For instance, it can be more significant in exterior regions of the molecule, like those exposed to the solvent, where NOE data can be insufficient. This could be the case for a bound ligand, for which coupling constants are a unique tool to determine local conformation via dihedral angles (consider also that for unlabeled ligands one cannot rely on parameters like residual dipolar couplings). Moreover, the experiment illustrated in this paper can also be used as a fast first assessment of the backbone structure of a bound ligand, long before the assignment of protein resonances is completed.

With our method a more general data treatment has been introduced whereby one can interpret the data in the presence of overlapping diagonal peaks, providing cross peaks are resolved. Moreover, data acquisition at two different total times for coupling evolution enables one to take into account the different relaxation properties of resonances giving rise to diagonal and cross peaks, directly when solving the equation system, without external assumptions. This more general approach guarantees a better control of the relative accuracy of the coupling constants and therefore translates into a more satisfactory control of the definition of the resulting structure.

References

- Barbato, G., Cicero, D.O., Nardi, M.C., Steinkühler, C., Cortese, R., De Francesco, R. and Bazzo, R. (1999) J. Mol. Biol., 289, 371–384.
- Barbato, G., Cicero, D.O., Cordier, F., Narjes, F., Gerlach, B., Sambucini, S., Grzesiek, S., Matassa, V.G., De Francesco, R. and Bazzo, R. (2000) EMBO J., 19, 1195–1206.
- Billeter, M., Neri, D., Otting, G., Qian, Y.Q. and Wüthrich, K. (1992) J. Biomol. NMR, 2, 257–274.
- Bystrov, V.F. (1976) Progr. NMR Spectrosc., 10, 41-81.
- Cicero, D.O., Barbato, G. and Bazzo, R. (1995) J. Am. Chem. Soc., 117, 1027–1033.

- Cicero, D.O., Barbato, G., Koch, U., Ingallinella, P., Bianchi, E., Nardi, M.C., Steinkühler, C., Cortese, R., Matassa, V., De Francesco, R., Pessi, A. and Bazzo, R. (1999) J. Mol. Biol., 289, 385–396.
- Dalvit, C., Cottens, S., Ramage, P. and Hommel, U. (1999) J. Biomol. NMR, 13, 43–50.
- Farrow, N., Muhandiram, D.R., Singer, A.U., Pascal, S.M., Kay, C.M., Gish, G., Shoelson, S.E., Pawson, T., Forman-Kay, J.D. and Kay, L.E. (1994) *Biochemistry*, 33, 5984–6003.
- Forman-Kay, J.D., Gronenborn, A.M., Kay, L.E., Wingfield, P.T. and Clore, M. (1990) *Biochemistry*, **29**, 1566–1572.
- Halgren, T.A. (1996) J. Comput. Chem., 17, 490–519.
- Harbison, G.S. (1993) J. Am. Chem. Soc., 115, 3026-3027.
- Heikkinen, S., Aitio, H., Permi, P., Folmer, R., Lappalainen, K. and Kilpeläinen, I. (1999) *J. Magn. Reson.*, **137**, 243–246.
- Ikura, M. and Bax, A. (1992) J. Am. Chem. Soc., 114, 2433–2440.
 Ingallinella, P., Bianchi, E., Ingenito, R., Koch, U., Steinkühler, C., Altamura, S. and Pessi, A. (2000) Biochemistry, 39, 12898–
- Karplus, M. (1959) J. Chem. Phys., 30, 11-15.
- Kay, L.E. and Bax, A. (1990) J. Magn. Reson., 86, 110-126.
- Kay, L.E., Nicholson, L.K., Delaglio, F., Bax, A. and Torchia, D.A. (1992) J. Magn. Reson., 97, 359–375.
- Keeler, J., Clowes, R.T., Davis, A.L. and Laue, E.D. (1994) Methods Enzymol., 239, 145–207.
- Kogler, H., Sørensen, O.W. and Ernst, R.R. (1983) J. Magn. Reson., 55, 157–163.
- Kuboniwa, H., Grzesiek, S., Delaglio, F. and Bax, A. (1994) J. Biomol. NMR, 4, 871–878.
- Löhr, F. and Rüterjans, H. (1995) J. Biomol. NMR, 5, 25-36.
- Lynden-Bell, R.M. (1967) Prog. NMR Spectrosc., 2, 163-204.
- Madsen, J.C., Sørensen, O.W., Sørensen, P. and Poulsen, F.M. (1993) J. Biomol. NMR, 3, 239–244.
- Permi, P., Kilpeläinen, I., Annila, A. and Heikkinen, S. (2000) J. Biomol. NMR, 16, 29–37.
- Postlingl, H. and Otting, G. (1998) *J. Biomol. NMR*, **12**, 319–324.

 Reyroth A. Schmidt P. Szalma S. Gennert T. Schwalbe H. and
- Rexroth, A., Schmidt, P., Szalma, S., Geppert, T., Schwalbe, H. and Griesinger, C. (1995) *J. Am. Chem. Soc.*, **113**, 10389–10390.
- Schechter, I. and Berger, A. (1967) Biochem. Biophys. Res. Commun., 27, 157–162.
- Sklenár, S. and Bax, A. (1987) J. Magn. Reson., 74, 469-479.
- Smallcombe, S.H., Patt, S.L. and Keifer, P.A. (1995) J. Magn. Reson., A117, 295–303.
- Vuister, G.W. and Bax, A. (1993) J. Am. Chem. Soc., 115, 7772–7777.
- Vuister, G.W., Kim, S.J. and Bax, A. (1994) J. Am. Chem. Soc., 116, 9206–9210.
- Weisemann, R., Rüterjans, H., Schwalbe, H., Schleucher, J., Bermel, W. and Griesinger, C. (1994) *J. Biomol. NMR*, 4, 231–240.